Bone 120 (2019) 487–494

Contents lists available at ScienceDirect

Bone

journal homepage: www.elsevier.com/locate/bone

Full Length Article

Bone adaptation compensates resorption when sciatic neurectomy is followed by low magnitude induced loading☆

Judith Piet[a], Dorothy Hu[c], Roland Baron[c], Sandra J. Shefelbine[a,b,*]

[a] Department of Bioengineering, Northeastern University, Boston, MA 02115, USA
[b] Department of Mechanical and Industrial Engineering, Northeastern University, Boston, MA 02115, USA
[c] Department of Medicine, Harvard Medical School, Division of Bone and Mineral Research, Department of Oral Medicine, Infection and Immunity, Harvard School of Dental Medicine, Boston, MA 02115, USA

ARTICLE INFO

Keywords:
Sciatic neurectomy
Axial loading
Bone adaptation
Histomorphometry

ABSTRACT

The uniaxial tibial loading model is commonly used to promote bone formation through mechanoadaptation in mice. Sciatic neurectomy on the other hand recruits osteoclasts, which results in bone loss. Previous studies have shown that combining sciatic neurectomy with high magnitude loading increases the amount of bone formed. Here we determine whether low-intensity loading (low magnitude and few cycles) is sufficient to maintain bone mass after sciatic neurectomy, either by promoting bone formation (balance between concurrent resorption and formation), or by preventing bone resorption altogether.

We examined bone adaptation in 4 groups of female C57BL/6J mice, 19–22 weeks old: (1) sham surgery +10 N loading; (2) sham surgery +5 N loading; (3) sciatic neurectomy; (4) sciatic neurectomy +5 N loading. Left legs were kept intact as internal controls. We examined changes in bone cross sectional properties and marrow area with micro-CT images, and histomorphometric measures with histological sections at the midpoint between tibiofibular junctions.

Loading at 10 N caused a significant increase in the amount of bone, but bone formation after 5 N of loading was not detectable in micro-CT images. There was significant bone loss in mice with sciatic neurectomy alone, but when combined with loading there was no significant bone loss. Histomorphometric analyses showed that loading at 5 N augmented bone formation periosteally on the lateral and posterior-medial surfaces, and reduced the number of endosteal osteoclasts on the posterior-medial surface compared to the contralateral leg. Combining sciatic neurectomy and loading at 5 N promoted faster mineral apposition on the periosteal lateral surface and augmented bone resorption on the endosteal posterior surface compared to the contralateral leg.

These data demonstrate that low-intensity loading is sufficient to maintain bone mass after sciatic neurectomy, both by preventing recruitment of osteoclasts on the endosteal surface and by compensating endosteal resorption caused by disuse with periosteal formation promoted by loading. This has implications for the loading required to maintain bone mass after injury or prolonged bedrest.

1. Introduction

Bone is a dynamic tissue, constantly adapting to external mechanical stimuli. High mechanical loads induce new bone formation, intermediate loads maintain bone mass, and disuse causes bone resorption [1]. Mechanoadaptation, the response of bones to mechanical loading, ensures that healthy mature bone remains strong enough to withstand elevated loads.

Many *in vivo* models have been developed to study the response of bone to mechanical loading (review of these models in [2]). A common model used to promote adaptation in mice is the uniaxial tibial loading model, in which an axial compressive load is placed across the knee and ankle [3–8]. This applies loading in a near-physiological direction and results in adaptation of both the cortical and trabecular bone, which can be evaluated by fluorescent labels and micro-computed tomography [7]. Though loading rate, number of cycles, and number of days of loading differ between studies using the murine tibial loading model, most studies have shown that the osteogenic response increases with load magnitude [9,10]. For very high load magnitudes, woven bone rather than lamellar bone forms, likely as a response to microcracking

☆ This research received internal funding from Northeastern University.
* Corresponding author at: Department of Bioengineering, Northeastern University, 805 Columbus Avenue, Boston, MA 02120, USA.
E-mail address: s.shefelbine@northeastern.edu (S.J. Shefelbine).

https://doi.org/10.1016/j.bone.2018.12.017
Received 13 September 2018; Received in revised form 21 December 2018; Accepted 21 December 2018
Available online 23 December 2018
8756-3282/

[11,12].

Studies have also examined the minimum load necessary to elicit an adaptive response, which is only evident with high resolution methods. The adaptive response was not evident at 6 N loading in mature females using micro-CT (26-week-old, 1200 cycles/day, 5 days/week for 2 weeks) [13], or at loads < 8.7 N using total interlabel area (20-week-old, 40 cycles/day, 3 days/week for 2 weeks) [7]. In the same studies, bone formation was achieved, mostly on the periosteal surface, for higher loads (11.5 N and 13 N respectively). When dynamic histomorphometry was examined separately on the endosteal and periosteal surfaces, an adaptive response was observed at 4.2 N (5-month-old, 1200 cycles/day, 5 days/week for 2 weeks), through the formation of periosteal lamellar bone. When loads were increased (5.5 N, 7 N), periosteal formation further increased, while the endosteal response was not consistent (no endosteal response observed at 4.2 N and 7 N, some endosteal response at 5.5 N) [10]. In younger animals, which are generally more responsive than mature animals, a 3 N load elicited an adaptive response (17-week-old, [14]). Combined, these studies indicate that in healthy mature bone, the amount of bone formed is correlated with the peak load and occurs mostly on the periosteal surface.

Several studies have tried to augment the amount of bone formed with pharmaceutical treatment. Short-term anti-resorptive treatment (Risedronate) did not alter the response of cortical and trabecular bone in mature female mice (17-week-old, [15]), which is unsurprising since the tibial loading model does not generally induce resorption. In mature female mice, high-dose PTH (1–34) combined with *in vivo* axial loading promoted more bone formation in the proximal tibia and distal ulna than loading or PTH alone (forming woven bone in the tibia) (13 to 19 weeks of age, [16]). Sclerostin is a protein that is down-regulated in response to mechanical loading. Sclerostin-antibody combined with loading promoted more cortical and trabecular bone formation than sclerostin-antibody or loading alone, in 10-week-old female mice [17].

Sciatic neurectomy is a common disuse model, which prompts bone loss in the neurectomized limb by increasing the number of osteoclasts and decreasing bone formation [18,19]. After four weeks of unilateral sciatic neurectomy, 13-week-old C57BL/6J mice had reduced bone formation and higher bone resorption on the tibial endocortical surface, compared to contralateral leg [20]. Tibiae collected three weeks following unilateral sciatic neurectomy had a higher medullar area and a lower cortical area compared to contralateral control bones, but the area enclosed within the periosteum was the same, indicating either reduced bone formation or augmented resorption on the endocortical surface (20-week-old female C57BL/6J mice) [21]. In 10-week-old C57BL/6J mice, 5 days of sciatic neurectomy reduced endosteal interlabel area along the tibia (proximal site, midshaft, and distal site) compared to mice with sham surgery, while periosteal interlabel area was reduced only at the distal site [22]. These studies indicate that in C57BL/6J mice, sciatic neurectomy reduces bone formation and increases bone resorption mostly on the endosteal surface.

Counterintuitively, sciatic neurectomy also augments the osteogenic response when combined with loading in mature bone [22]. Sclerostin upregulation caused by disuse after neurectomy was reversed with axial tibial loading, resulting in fewer sclerostin-positive osteocytes in the neurectomized, loaded bone than in the contralateral tibia, analyzed at a few select sites [23]. These studies used loads of 10–13 N, which is sufficient for an adaptive response in mature bone, and when combined with sciatic neurectomy increased the endosteal and periosteal interlabel area. Further gene arrays showed differential gene expression after sciatic neurectomy and loading compared to loading alone [24]. Interestingly in old bone (> 19 months), which is less mechanoresponsive than mature bone [13,14,25–27], sciatic neurectomy was able to restore the adaptive response to levels seen in young mice [28].

These studies indicate a synergistic effect of sciatic neurectomy and loading, but do not indicate the mechanism responsible for the augmented response. It is also not clear if low levels of loading are rendered sufficient for mechanoadaptation after sciatic neurectomy. Dose-response curves for mature mice with sciatic neurectomy and loading indicate no increase in cortical bone area at low magnitude loads (2 N–6 N) [28,29]. However, for these magnitudes, these studies did not use histomorphometry to track bone formation and resorption. It is therefore unclear if low magnitude loading was insufficient to promote bone formation, if bone formation could not be detected by micro-CT images, or if bone formation and resorption occurred simultaneously on different surfaces.

In this paper, we probe the combined effects of sciatic neurectomy, which promotes resorption, and loading, which promotes formation, to determine if low magnitude loads are sufficient to maintain bone mass. Bone mass may be preserved by inhibiting resorption, or balancing resorption with increased formation. Because resorption primarily occurs endosteally and formation primarily occurs periosteally, we hypothesize that bone mass is conserved by the summative effect of endosteal resorption induced by sciatic neurectomy, and of periosteal formation induced by low amounts of loading. With X-ray computed tomography and histomorphometry, we examine whether low magnitude loads prevent bone loss by inhibiting bone resorption, or promote bone formation on a background of disuse (concurrent increase in bone formation and resorption on different bone surfaces).

2. Material and methods

2.1. Animals

Female C57BL/6J mice were purchased at 7–10 weeks of age from Jackson Laboratory and aged until 16–19 weeks old. Animals were housed in groups of five, fed *ad libitum* with maintenance mouse diet and subjected to a 12-h light/dark cycle. All procedures received approval from the Northeastern University's Institutional Animal Care and Use Committee (IACUC). We examined 4 groups of mice with sciatic neurectomy or sham surgery and tibial loading at different magnitudes (Fig. 1A): (1) **sham surgery + 10 N** loading is s to be osteogenic in previous studies [7] (n = 5); (2) **sham surgery + 5 N loading** is expected to be insufficient to induce mechanoadaptation [7] (n = 5); (3) **sciatic neurectomy** determines the effect of disuse alone (n = 7); (4) **sciatic neurectomy + 5 N** loading determines if low-intensity bouts of loading preserve bone (n = 7). Mice were sacrificed at 19–22 weeks of age. An additional group of slightly older mice (26 weeks, n = 5) was sacrificed 5 days following surgery (results are presented as Supplementary Data because age does not exactly match other groups).

2.2. Sciatic neurectomy and sham surgery

At 16–19 weeks of age, on day 0, mice were anesthetized with 5% isofluorane, and the sciatic nerve of the right hindlimb was sectioned (or left intact in the sham surgery group) (procedure described in [30]). The biceps femori and skin were closed, and sutures were reinforced with Vetbond (3 M). Mice were administered Buprenex (0.05 mg/kg) subcutaneously, twice a day until day 3.

2.3. Mechanical loading

Starting on day 5, mice were subjected to *in vivo* axial tibial loading, three days a week for two weeks (Fig. 1A). Under isofluorane induced anesthesia, the right knee and ankle were placed in custom made loading cups and held with a preload of 2 N. The right tibia was subjected to 100 cycles of compressive loading at a peak load of 5 N or 10 N, with a rise and unloading rate of 45–65 N/s and 1 s rest period between each cycle (Instron 5942) (Fig. 1B).

2.4. Fluorescent labelling

Mice were injected with fluorescent labels. On days 3 and 4, a dose

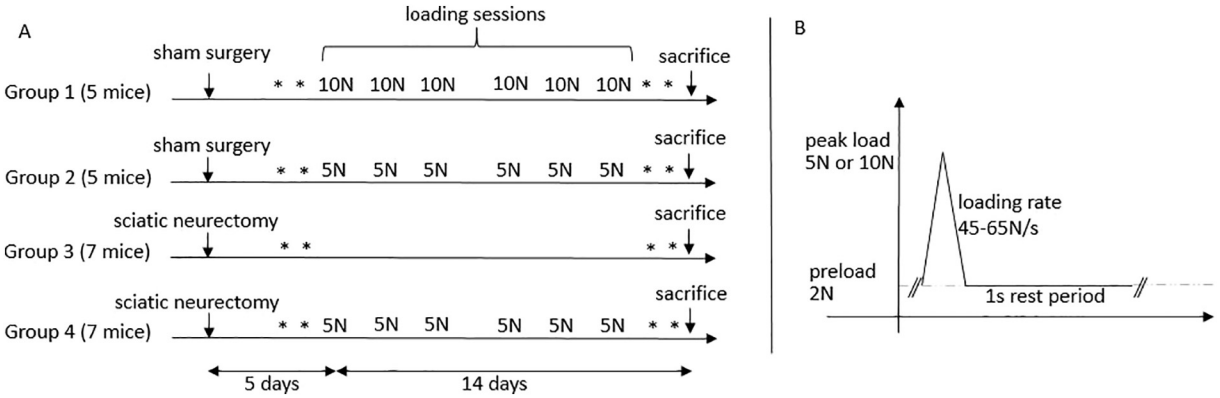

Fig. 1. Experimental protocol: A) Experimental schedule. 10 N: repeated cyclic loading at 10 N peak load; 5 N: repeated cyclic loading at 5 N peak load. * indicates injection of fluorochrome labels; B) *In vivo* cyclic loading profile: each cycle is repeated 100 cycles/day, 3 days/week for 2 weeks.

of 20 mg/kg calcein (Sigma C0875) was injected intraperitoneally. On days 17 and 18, a dose of 40 mg/kg demeclocycline (Sigma D6140) and 10 mg/kg calcein was injected.

2.5. Sacrifice and bone fixation

Mice were sacrificed 19 days following surgery by CO_2 inhalation and cervical dislocation. Immediately after sacrifice, tibiae of both left and right hind limbs were carefully dissected, fixed in 70% ethanol, and stored at 4 °C until scanning.

2.6. Microtomography

The left and right tibiae were scanned (10 µm resolution, 55 kV, 145 µA, Scanco µCT 35). Using the BoneJ plugin in ImageJ [31], we measured bone area (cortical and trabecular area) for each slice. We then obtained the change in bone area in the right treated leg, relative to the left control leg, between the tibiofibular junctions (from 0% at the proximal tibiofibular junction, to 100% at the distal tibiofibular junction). We define tibiofibular junctions as the locations where the tibia and the fibula split on micro-CT images (at 9% and 61% of total tibial length). We also segmented out the medullar area using Mimics (Materialise NV) and obtained relative changes in medullar area along the tibia, between the tibiofibular junctions. We analyzed changes in bone or medullar area using spm1d [32], a package for one-dimensional Statistical Parametric Mapping [33], using two-tailed one-sample *t*-tests, with the null hypothesis that the relative change in bone area (or medullar area) equals zero. Spm1d uses random field theory to make statistical inferences in normalized sets of 1D measurements.

2.7. Histomorphometry

After microtomography imaging, tibiae were embedded in methylmetacrylate (MMA). 4-µm sections were cut in diaphyseal midshaft, at the midpoint between proximal and distal tibio-fibular junctions (RM2255, Leica Biosystems, IL, USA) (Fig. 2A). Cutting sections as thin as 4-µm enhances cell visualization (osteoblasts and osteoclasts in particular). For each bone, one slide was left unstained for the measurement of endocortical and periosteal dynamic parameters with injected-fluorochrome labeling, one slide was stained with tartrate-resistant acid phosphatase (TRAP), and one slide was stained with 2% toluidine blue for the measurement of endocortical static histomorphometry parameters. Periosteal static histomorphometry parameters were not assessed, because soft tissue removal after sacrifice, required for proper MMA embedding, usually damages the periosteal surface. The periosteal surface was analyzed for fluorochrome labels. Each histological section was divided into 4 zones: 1) posterior; 2) lateral, 3) anterior-medial, and 4) posterior-medial (Fig. 2B).

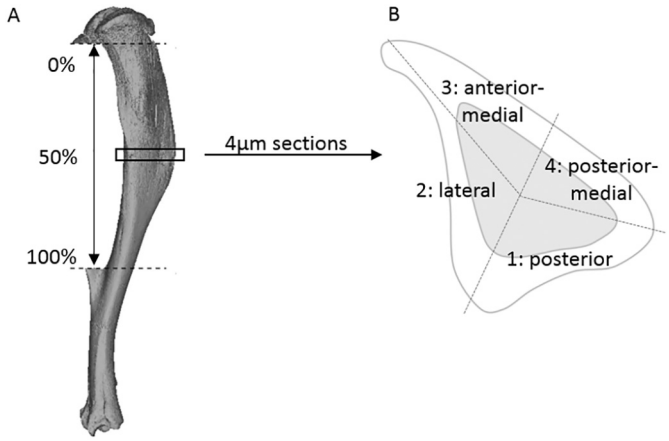

Fig. 2. A) Cross sectional parameters were assessed along the length of the bone from proximal tibiofibular junction (0%) to distal tibiofibular junction (100%). B) Histomorphometric analysis of fluorescent labels and cellular parameters were performed at 50%. All histomorphometric parameters were assessed in each of 4 zones both endosteally and periosteally.

For each zone, dynamic parameters mineral apposition rate (MAR) and mineralizing surface per bone surface (MS/BS) were measured with the OsteoMeasure analyzing system (Osteometrics Inc., Decatur, GA, USA) at 200× magnification, in unstained sections both on the periosteal (Ps.) and endocortical (Ec.) bone surface (Ps.MAR, Ec.MAR, Ps.MS/BS and Ec.MS/BS). The bone formation rate (Ps.BFR and Ec.BFR) was calculated with the product of MAR and MS/BS. The static histomorphometry parameters, number of osteoblasts (N.Ob), osteoid surface per bone surface (OS/BS), and number of osteoclasts (N.Oc), were measured on endocortical surfaces.

In each group, we compared, for each of the zones, a parameter's mean value in the right treated tibiae *versus* in the contralateral sections (using two-tailed paired *t*-tests). We can then report the increase or decrease of histomorphometric parameters caused by treatment, in each zone, compared to the contralateral control leg in the same animal.

3. Results

3.1. Microtomography

When comparing the contralateral (left) tibiae in all 4 groups using 1D statistical parametric mapping, with a one-way analysis of variance test (ANOVA) on the average bone area within each group, we find that no group is different from the others (in particular, the left tibiae in the group with sciatic neurectomy are no different from the left tibiae in

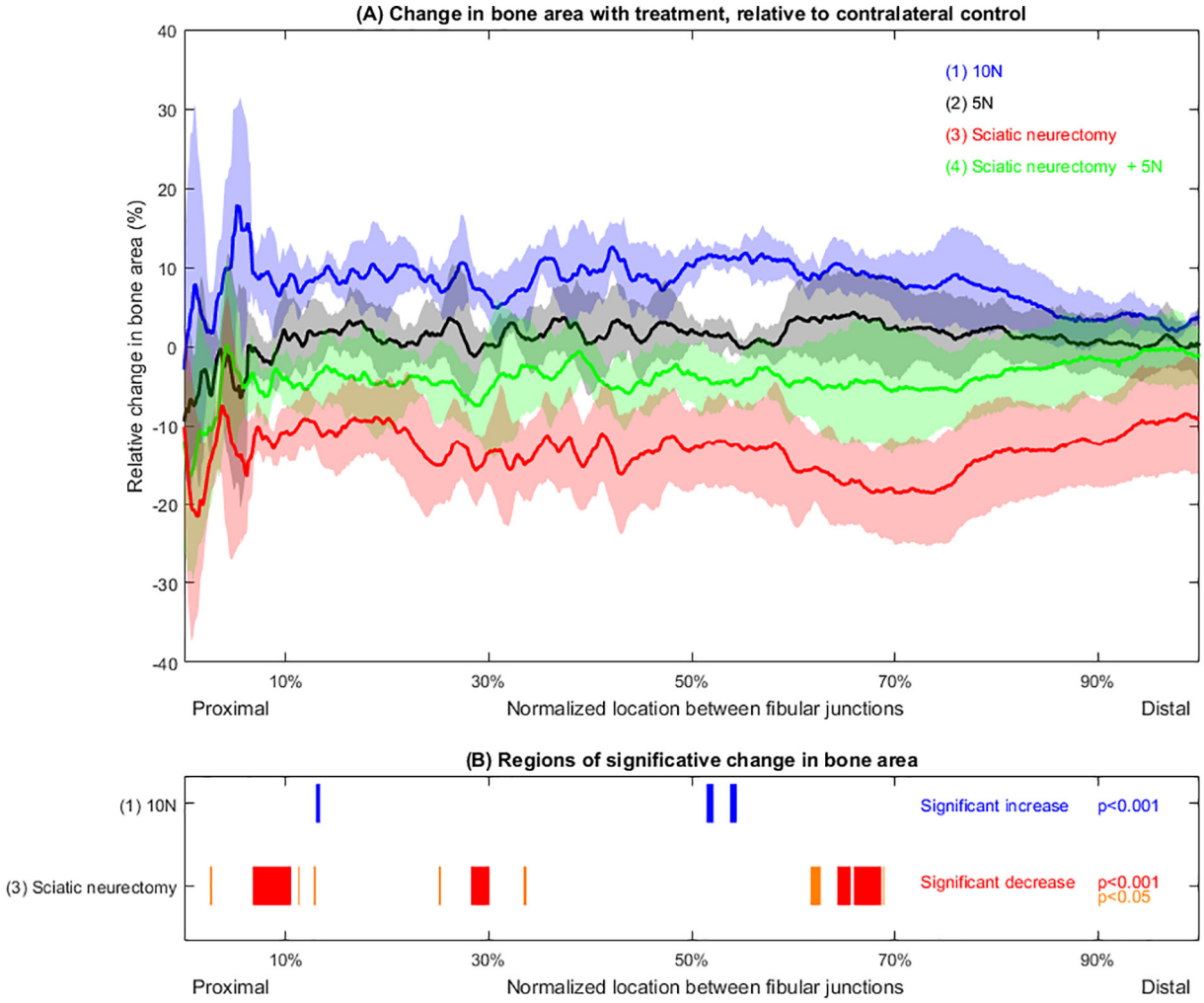

Fig. 3. A) Change in cortical bone area with treatment, relative to the contralateral tibia, along the normalized location between tibiofibular junctions in all groups, presented as mean (solid line) and standard deviation (shaded area). B) Location and cluster p-values for regions of significant changes in bone area, according to micro-CT images. No significant changes were observed for group 2 and 4 (5 N and sciatic neurectomy + 5 N). Statistical significance was tested with 1D Statistical Parametric Mapping, using two-tailed one-sample *t*-tests, with the null hypothesis that mean relative change in bone area equals zero.

other groups) (Supplementary Fig. S2). We find therefore that it is appropriate to report changes relative to the contralateral tibiae.

Loading bones at 10 N peak load caused a significant increase in bone mass at different sites (Fig. 3, group 1). Loading bones at 5 N peak load did not cause a significant change in bone area in micro-CT images (Fig. 3, group 2). Mice sacrificed 19 days following sciatic neurectomy exhibited a decrease in bone area at different sites (Fig. 3, group 3). When sciatic neurectomy was followed by sessions of loading at 5 N peak load, changes in bone area were prevented (no significant changes, Fig. 3, group 4), suggesting that either resorption was prevented, or resorption and formation occurred in balance.

As a result of active resorption, the medullar area was significantly increased in mice sacrificed 19 days following sciatic neurectomy (group 3, increase localized at 60% and 70% of the normalized tibial length, data not shown). In all other groups, including the mice with sciatic neurectomy + 5 N load, no change in medullar area was observed, suggesting that 5 N loading prevented the net bone loss induced by sciatic neurectomy.

3.2. Histomorphometry

In order to better understand the mechanisms by which 5 N loading prevented bone loss after sciatic neurectomy, we analyzed the samples using histomorphometry. We examined the 5 N loaded group (group 2) to determine if there was bone formation detectable with higher resolution histomorphometry, despite being undetectable with micro-CT; the group that was sacrificed 19 days following neurectomy (group 3) to determine the effects of neurectomy alone; and the sciatic neurectomy + 5 N group (group 4) to determine if bone resorption was inhibited or if there was concurrent bone resorption and formation. Histomorphometry was not performed on group 1 as micro-CT images indicated an increase in bone formation, and standard loading has been well documented with dynamic histomorphometry in previous studies [7,10].

In all groups, we noticed a steady-state anterior-to-posterior drift on the contralateral control leg (left tibiae, Fig. 4A), with resorption on the anterior periosteal surface (jagged resorption surface in zone 4) and formation on the posterior periosteal surface (single or double label in zone 1). All changes in the right leg were measured relative to this baseline drift in the left leg (Fig. 6).

Loading at 5 N (right leg) increased periosteal mineralizing surface and bone formation rate for zone 2 (lateral surface), increased mineralizing surface for zone 4 (posterior-medial surface) (Fig. 4), and decreased the endosteal quantity of osteoclasts on zone 4 (Fig. 6A).

Sciatic neurectomy for 19 days induced an increase in osteoclasts on the endosteal surface of zones 1 and 2 (posterior and lateral surfaces), a decrease in periosteal mineralizing surface on zone 1 (posterior surface), and a decrease in endosteal mineralizing surface for zones 1, 2

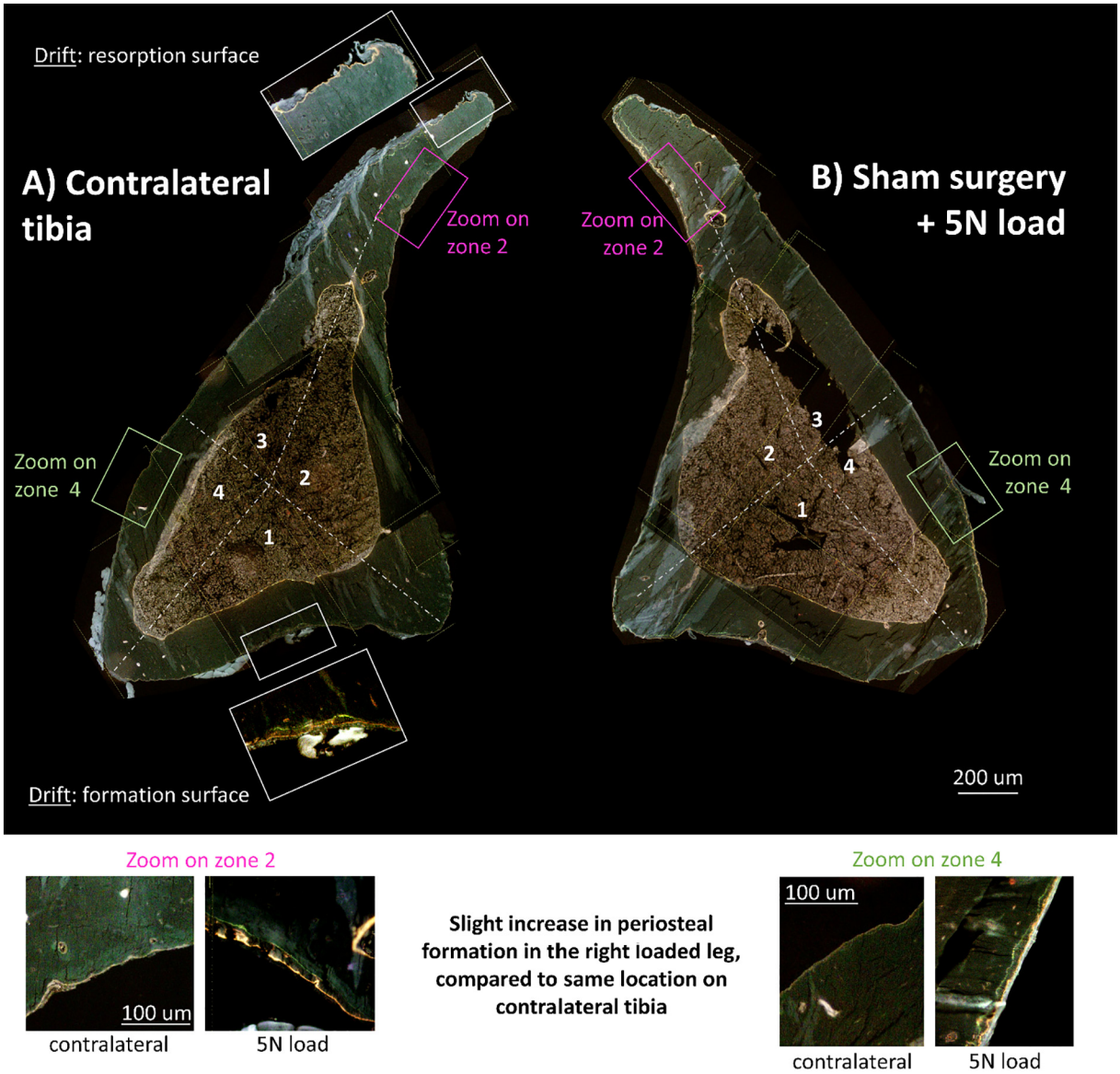

Fig. 4. Fluorescent labels in representative histological sections taken at 50% of the tibial length normalized between tibiofibular junctions of A) contralateral control limb; B) sham surgery and loading at 5 N. The boxes highlight remarkable patterns, with a zoomed in view of the region of interest. The contralateral tibia presents a typical drift from the anterior surface (resorption on the periosteal surface of zone 3) to the posterior surface (double labels on the periosteal surface on zone 1) (white boxes). The right treated tibia presents a slight increase in mineralizing surface on the lateral and medial surfaces (double labels on the periosteal surfaces on zone 2 and 4), as illustrated by the inset pictures.

and 4 (posterior, lateral and posterior-medial) (Fig. 6B).

Combining sciatic neurectomy and loading at 5 N promoted increased bone formation and increased bone resorption on different surfaces of the treated tibia (right leg) (Fig. 5). In zone 2 (lateral surface), there was an increase in the periosteal mineral apposition rate and bone formation rate, as well as in the endosteal osteoid perimeter. Concurrently, the number of osteoclasts increased on the endosteal surface of zone 1 (posterior side), and the mineralizing surface and mineral apposition rate decreased on the endosteal surface of zone 4 (posterior-medial surface) (Figs. 5 and 6C).

In all groups the right (treated) leg was significantly different from the left control, in multiple zones (Fig. 6). All parameters are reported in detail in the Supplementary Data.

4. Discussion

This study uses micro-computed tomography and surface-specific histomorphometry (examining different surfaces of each cross section) to analyze the effects of sciatic neurectomy and low levels of loading on mature bone (5 N, 100 cycles, 3 days/week for 2 weeks).

Loading at 10 N caused a localized increase in bone area (at 52–54% of the normalized location on tibia). This corresponds to 36–37% of the whole tibia, which is where the greatest adaptive response to axial loading has previously been observed [16,34–38].

Despite micro-computed images showing no change in bone cross sectional geometry with 5 N loading, and with sciatic neurectomy followed by 5 N loading, histomorphometric results provide more specific, higher resolution information on bone status. Even low levels of loading were sufficient to promote some adaptation (on the periosteal posterior-medial and lateral surfaces). This amount of loading was also sufficient to maintain the amount of bone following sciatic neurectomy by balancing bone resorption on the posterior endosteal surface, and increased bone formation and mineral apposition rates on the lateral periosteal surface.

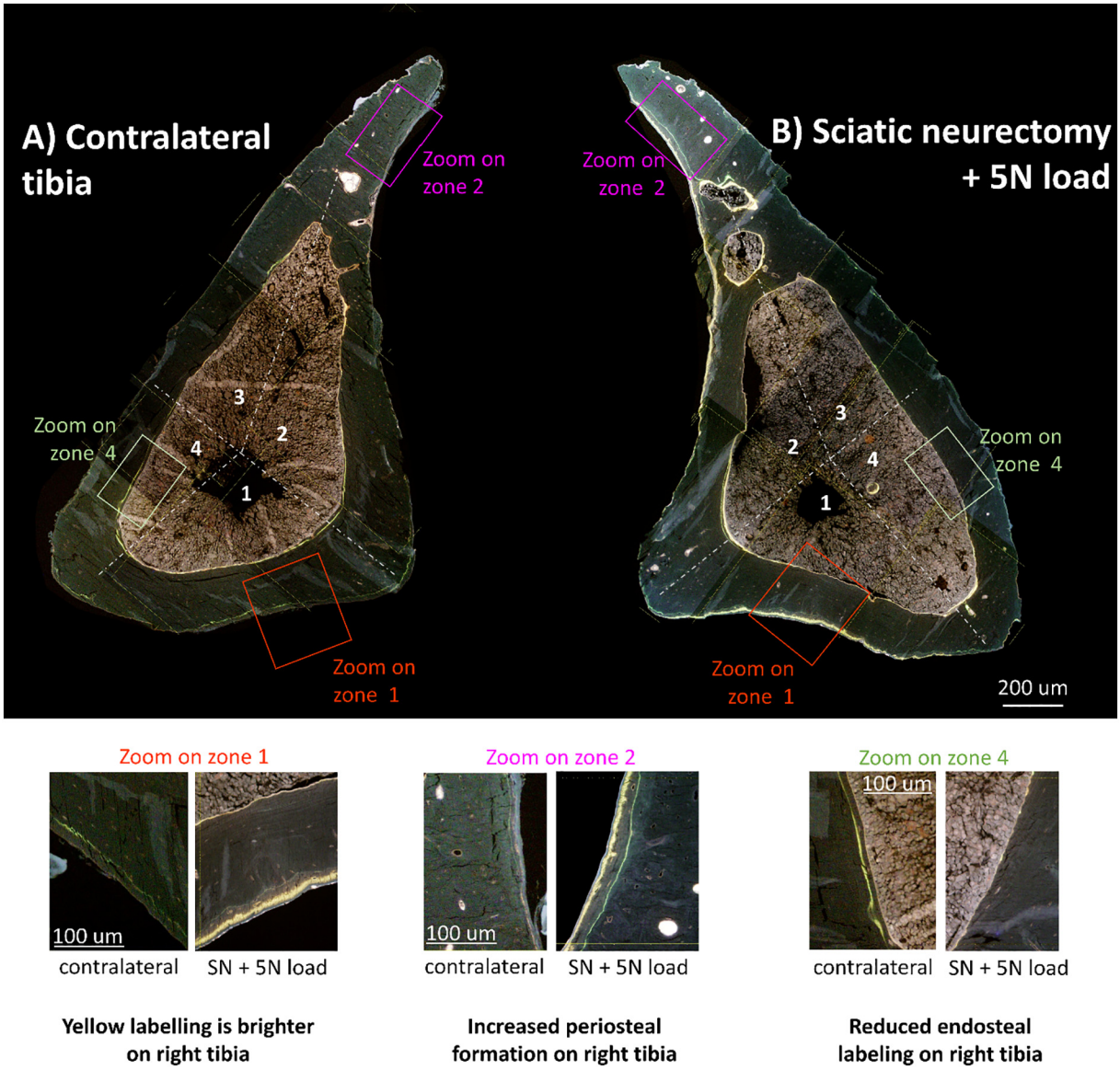

Fig. 5. Fluorescent labels in representative histological sections from the midshaft of A) contralateral control limb; B) sciatic neurectomy and loading at 5 N. The treated right leg displays a bright and broad yellow labeling on the periosteal posterior surface (zone 1, calcein + demeclocycline, injected before sacrifice). Periosteal bone formation is increased on the lateral surface (zone 2), while endosteal mineralizing surface is decreased on the medial surface (zone 4). (For interpretation of the references to colour in this figure legend, the reader is referred to the web version of this article.)

Low magnitude loading with an intensive regimen (4 N, 1200 cycles, 5 days/week for 2 weeks, triangular pulse, 49-100 N/s, 0.1 s rest period), which is 20 times the number of loading cycles we used, has been shown to increase bone formation the periosteal surface [10]. For low magnitude loading regimens that are not as intensive (2–6 N, 40 cycles, 3 days/week, triangular pulse, 28–44 N/s, 10 s rest period), micro-CT images and classic histomorphometry averaged across the whole cross-section show no increase in bone formation [7]. However, we show that even a low magnitude loading (5 N, 100 cycles/day, 3 days/week, triangular pulse, 45–65 N/s, 1 s rest period) can induce bone formation on the lateral and posterior-medial surfaces, which can only be detected by surface-specific histomorphometry.

Several studies report a synergistic effect of sciatic neurectomy and loading, but have used significantly higher loads (10–14 N) in mature females [22,23,28]. At lower load magnitudes (3–6 N), sciatic neurectomy combined with loading resulted in a decrease in bone cross sectional area [28,29]. In these dose response studies, peak loads of 8 N, 40 cycles/day, 3 times/week for 2 weeks, were required to maintain cortical and trabecular bone mass in mice with sciatic neurectomy (triangular pulse, 28–44 N/s, 10 s rest period in [22], trapezoidal pulse with 0.05 s hold, 500 N/s, 10 s rest in [23,28,29]). We found that 5 N, 100 cycles/day, 3 times/week for 2 weeks, was sufficient to maintain bone mass. There is likely a balance between magnitude of load and number of loading cycles required to maintain bone. Previous studies did not conduct histomorphometric analysis of the low magnitude loads, and it was therefore unclear whether bone mass was preserved by inhibiting resorption, or a combination of bone formation and resorption simultaneously on different surfaces. In this study, we demonstrate that bone formation occurs even at low magnitude loads, and that a few loading cycles are sufficient to maintain bone mass after neurectomy. The distribution of bone mass changes as resorption occurs endosteally on the posterior surface and formation occurs periosteally, particularly on the lateral surface.

Previous studies hypothesized that lack of background loading “sensitized” the bone [23,28,29], but a mechanism was not provided. We show that loading at 5 N decreased the number of endosteal

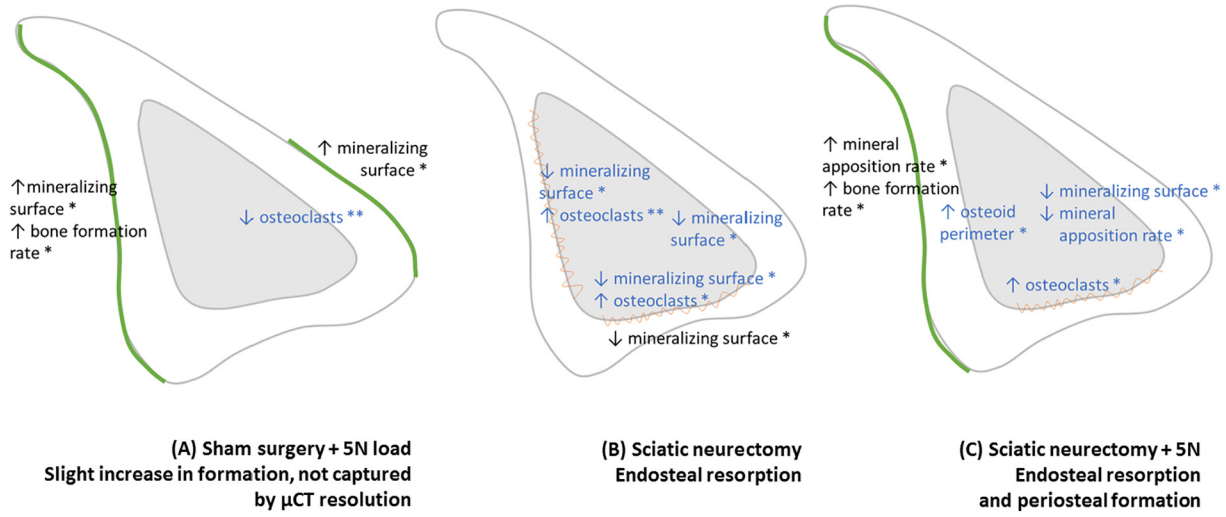

Fig. 6. Summary of histomorphometric data, presented as significant changes in right tibiae, relative to contralateral controls. Student's two-tailed paired *t*-tests, comparing left control tibia to right treated tibia. (A) Group with sham surgery + 5 N load; (B) Group with sciatic neurectomy; (C) Group with sciatic neurectomy + 5 N load. Periosteal parameters are reported in black, endosteal parameters are reported in blue.
Green line: surface of increased bone formation; red jagged line: surface of increased bone resorption, compared to contralateral tibiae. * $p < 0.05$; ** $p < 0.01$. (For interpretation of the references to colour in this figure legend, the reader is referred to the web version of this article.)

osteoclasts (on the medial-posterior surface). Sciatic neurectomy for 19 days-resulted in an increase in osteoclasts on the posterior and lateral endosteal surfaces. When both sciatic neurectomy and loading were combined, loading prevented the disuse-related increase in osteoclasts on the lateral surface, but resorption still occurred on the posterior surface.

Because muscles were dissected before bone fixation, we cannot provide reliable data on periosteal cells. In the future, we will keep surrounding muscles before limb fixation.

In the group with sciatic neurectomy and loading, the amount of bone was conserved *via* two mechanisms: (1) the accumulation of osteoclasts on the endosteal lateral surface was prevented; (2) there was simultaneous resorption on the endosteal posterior surface, and an increased rate of mineral apposition on the periosteal lateral surface.

In the group that had sciatic neurectomy only, osteoclasts accumulated on the lateral endosteal surface. Osteocytes respond to unloading by releasing increased levels of RANKL and sclerostin [39,40]. Sclerostin inhibits osteoblast differentiation, while RANKL promotes osteoclast differentiation and function. Loading, on the contrary, reduces the expression of sclerostin by osteocytes [40]. *In vitro* experiment have shown that mechanical stimulation of osteocytes by strain-derived fluid flow results in the production of nitric oxide, which induces osteoclast apoptosis and suppresses osteoclast activity, and of PGE2, which promotes osteoblast differentiation [41–44]. In summary, the effects of combining neurectomy with loading are region specific. On the lateral surface, where osteocytes receive the greatest mechanical signal during loading [45], resorption is inhibited and formation is promoted. On the posterior surface where the mechanical signal from loading is low (because it is near the neutral axis), resorption occurs.

We applied the same magnitude of loading to the neurectomized and sham surgery groups. To ensure that the mechanical stimulus was similar, we examined a group of mice five days after sciatic neurectomy, which corresponds to the start of loading. This group had no change in cross sectional area, minimum and maximum moments of area, or cortical thickness between the neurectomized leg and the contralateral leg (Supplementary Figs. S5 and S6), indicating that 5 days of neurectomy does not significantly affect the bone geometry (though underpowered, $p = 0.2176$; power = 0.2053 for the cortical thickness at the location where histomorphometry is performed, 21 animals would be needed to achieve a power of 0.8). Our previous modeling [45] and strain mapping studies [46] have indicated that the change in shape (periosteal apposition and endosteal resorption) that occurs during aging is responsible for the differences in surface strain at different ages under the same load. Because we found no change in shape after 5 days, 5 N loading likely produced the same cortical strains in both the control group and neurectomized group.

We would like to emphasize the importance of region-specific histomorphometry to capture histomorphometric differences within a cross section. Averaging endosteal and periosteal histomorphometric results on the whole cross-sectional was unable to capture the different status of separate cortical surfaces. Region-specific histomorphometry also enabled us to capture general behavior in the contralateral bones, such as the drift from the anterior to the posterior surface, which is averaged out if analyzed across the entire surface.

These results demonstrate that low magnitude loads can maintain bone mass after sciatic neurectomy, by balancing resorption caused by disuse and formation promoted by loading in different regions of the bone, and by preventing the recruitment of osteoclasts on other endosteal surfaces. This might have implications for the physical therapy required to maintain bone mass during prolonged unloading, such as bedrest or injury.

Declarations of interest

None.

Appendix A. Supplementary data

Supplementary data to this article can be found online at https://doi.org/10.1016/j.bone.2018.12.017.

References

[1] H.M. Frost, Bone "mass" and the "mechanostat": a proposal, Anat. Rec. 219 (1987) 1–9, https://doi.org/10.1002/ar.1092190104.
[2] L.B. Meakin, J.S. Price, L.E. Lanyon, The contribution of experimental in vivo models to understanding the mechanisms of adaptation to mechanical loading in bone, Front. Endocrinol. 5 (2014), https://doi.org/10.3389/fendo.2014.00154.
[3] J. Fritton, E. Myers, T. Wright, M. Van Der Meulen, Loading induces site-specific increases in mineral content assessed by microcomputed tomography of the mouse tibia, Bone 36 (2005) 1030–1038, https://doi.org/10.1016/j.bone.2005.02.013.
[4] B.M. Willie, A.I. Birkhold, H. Razi, T. Thiele, M. Aido, B. Kruck, et al., Diminished response to in vivo mechanical loading in trabecular and not cortical bone in adulthood of female C57Bl/6 mice coincides with a reduction in deformation to

load, Bone 55 (2013) 335–346, https://doi.org/10.1016/j.bone.2013.04.023.
[5] H. Yang, K.D. Butz, D. Duffy, G.L. Niebur, E.A. Nauman, R.P. Main, Characterization of cancellous and cortical bone strain in the in vivo mouse tibial loading model using microCT-based finite element analysis, Bone 66 (2014) 131–139, https://doi.org/10.1016/j.bone.2014.05.019.
[6] L.K. Saxon, B.F. Jackson, T. Sugiyama, L.E. Lanyon, J.S. Price, Analysis of multiple bone responses to graded strains above functional levels, and to disuse, in mice in vivo show that the human Lrp5 G171V High Bone Mass mutation increases the osteogenic response to loading but that lack of Lrp5 activity reduces it, Bone 49 (2011) 184–193, https://doi.org/10.1016/j.bone.2011.03.683.
[7] R.L. De Souza, M. Matsuura, F. Eckstein, S.C.F. Rawlinson, L.E. Lanyon, A.A. Pitsillides, Non-invasive axial loading of mouse tibiae increases cortical bone formation and modifies trabecular organization: a new model to study cortical and cancellous compartments in a single loaded element, Bone 37 (2005) 810–818, https://doi.org/10.1016/j.bone.2005.07.022.
[8] M.D. Brodt, C.B. Ellis, M.J. Silva, Growing C57Bl/6 mice increase whole bone mechanical properties by increasing geometric and material properties, J. Bone Miner. Res. 14 (1999) 2159–2166, https://doi.org/10.1359/jbmr.1999.14.12.2159.
[9] A.M. Weatherholt, R.K. Fuchs, S.J. Warden, Cortical and trabecular bone adaptation to incremental load magnitudes using the mouse tibial axial compression loading model, Bone 52 (2013) 372–379, https://doi.org/10.1016/j.bone.2012.10.026.
[10] D. Sun, M.D. Brodt, H.M. Zannit, N. Holguin, M.J. Silva, Evaluation of loading parameters for murine axial tibial loading: stimulating cortical bone formation while reducing loading duration, J. Orthop. Res. (2017), https://doi.org/10.1002/jor.23727.
[11] J.A. McKenzie, E.C. Bixby, M.J. Silva, Differential gene expression from microarray analysis distinguishes woven and lamellar bone formation in the rat ulna following mechanical loading, Beier F, editor, PLoS One 6 (2011) e29328, , https://doi.org/10.1371/journal.pone.0029328.
[12] S.H. McBride, M.J. Silva, Adaptive and injury response of bone to mechanical loading, Bonekey Rep. 1 (2012) 192, https://doi.org/10.1038/bonekey.2012.192.
[13] M.E. Lynch, R.P. Main, Q. Xu, T.L. Schmicker, M.B. Schaffler, T.M. Wright, et al., Tibial compression is anabolic in the adult mouse skeleton despite reduced responsiveness with aging, Bone 49 (2011) 439–446, https://doi.org/10.1016/j.bone.2011.05.017.
[14] L.B. Meakin, G.L. Galea, T. Sugiyama, L.E. Lanyon, J.S. Price, Age-related impairment of bones' adaptive response to loading in mice is associated with sex-related deficiencies in osteoblasts but no change in osteocytes, J. Bone Miner. Res. 29 (2014) 1859–1871, https://doi.org/10.1002/jbmr.2222.
[15] T. Sugiyama, L.B. Meakin, G.L. Galea, B.F. Jackson, L.E. Lanyon, F.H. Ebetino, et al., Risedronate does not reduce mechanical loading-related increases in cortical and trabecular bone mass in mice, Bone 49 (2011) 133–139, https://doi.org/10.1016/j.bone.2011.03.775.
[16] T. Sugiyama, L.K. Saxon, G. Zaman, A. Moustafa, A. Sunters, J.S. Price, et al., Mechanical loading enhances the anabolic effects of intermittent parathyroid hormone (1–34) on trabecular and cortical bone in mice, Bone 43 (2008) 238–248, https://doi.org/10.1016/j.bone.2008.04.012.
[17] A. Morse, A. Schindeler, M.M. McDonald, M. Kneissel, I. Kramer, D.G. Little, Sclerostin antibody augments the anabolic bone formation response in a mouse model of mechanical tibial loading, J. Bone Miner. Res. 33 (2018) 486–498, https://doi.org/10.1002/jbmr.3330.
[18] A. Sakai, T. Mori, M. Sakuma-Zenke, T. Takeda, K. Nakai, Y. Katae, et al., Osteoclast development in immobilized bone is suppressed by parathyroidectomy in mice, J. Bone Miner. Metab. 23 (2005) 8–14, https://doi.org/10.1007/s00774-004-0534-y.
[19] M. Weinreb, G.A. Rodan, D.D. Thompson, Osteopenia in the immobilized rat hind limb is associated with increased bone resorption and decreased bone formation, Bone 10 (1989) 187–194, https://doi.org/10.1016/8756-3282(89)90052-5.
[20] Y. Kodama, H. Dimai, J. Wergedal, M. Sheng, R. Malpe, S. Kutilek, et al., Cortical tibial bone volume in two strains of mice: effects of sciatic neurectomy and genetic regulation of bone response to mechanical loading, Bone 25 (1999) 183–190, https://doi.org/10.1016/S8756-3282(99)00155-6.
[21] G.L. Galea, S. Hannuna, L.B. Meakin, P.J. Delisser, L.E. Lanyon, J.S. Price, Quantification of alterations in cortical bone geometry using site specificity software in mouse models of aging and the responses to ovariectomy and altered loading, Front. Endocrinol. 6 (2015), https://doi.org/10.3389/fendo.2015.00052.
[22] R.L. De Souza, A.A. Pitsillides, L.E. Lanyon, T.M. Skerry, C. Chenu, Sympathetic nervous system does not mediate the load-induced cortical new bone formation, J. Bone Miner. Res. 20 (2005) 2159–2168, https://doi.org/10.1359/JBMR.050812.
[23] A. Moustafa, T. Sugiyama, J. Prasad, G. Zaman, T.S. Gross, L.E. Lanyon, et al., Mechanical loading-related changes in osteocyte sclerostin expression in mice are more closely associated with the subsequent osteogenic response than the peak strains engendered, Osteoporos. Int. 23 (2012) 1225–1234, https://doi.org/10.1007/s00198-011-1656-4.
[24] G. Zaman, L.K. Saxon, A. Sunters, H. Hilton, P. Underhill, D. Williams, et al., Loading-related regulation of gene expression in bone in the contexts of estrogen deficiency, lack of estrogen receptor α and disuse, Bone 46 (2010) 628–642, https://doi.org/10.1016/j.bone.2009.10.021.
[25] N. Holguin, M.D. Brodt, M.E. Sanchez, M.J. Silva, Aging diminishes lamellar and woven bone formation induced by tibial compression in adult C57BL/6, Bone 65 (2014) 83–91, https://doi.org/10.1016/j.bone.2014.05.006.
[26] S. Srinivasan, B.J. Ausk, J. Prasad, D. Threet, S.D. Bain, T.S. Richardson, et al., Rescuing loading induced bone formation at senescence, Judex S, editor, PLoS Comput. Biol. 6 (2010) e1000924, , https://doi.org/10.1371/journal.pcbi.1000924.
[27] R.P. Main, M.E. Lynch, M.C.H. van der Meulen, Load-induced changes in bone stiffness and cancellous and cortical bone mass following tibial compression diminish with age in female mice, J. Exp. Biol. 217 (2014) 1775–1783, https://doi.org/10.1242/jeb.085522.
[28] L.B. Meakin, P.J. Delisser, G.L. Galea, L.E. Lanyon, J.S. Price, Disuse rescues the age-impaired adaptive response to external loading in mice, Osteoporos. Int. 26 (2015) 2703–2708, https://doi.org/10.1007/s00198-015-3142-x.
[29] T. Sugiyama, L.B. Meakin, W.J. Browne, G.L. Galea, J.S. Price, L.E. Lanyon, Bones' adaptive response to mechanical loading is essentially linear between the low strains associated with disuse and the high strains associated with the lamellar/woven bone transition, J. Bone Miner. Res. 27 (2012) 1784–1793, https://doi.org/10.1002/jbmr.1599.
[30] J.A.E. Batt, J.R. Bain, Tibial nerve transection - a standardized model for denervation-induced skeletal muscle atrophy in mice, J. Vis. Exp. (2013) e50657, https://doi.org/10.3791/50657.
[31] M. Doube, M.M. Kłosowski, I. Arganda-Carreras, F.P. Cordelières, R.P. Dougherty, J.S. Jackson, et al., BoneJ: free and extensible bone image analysis in ImageJ, Bone 47 (2010) 1076–1079, https://doi.org/10.1016/j.bone.2010.08.023.
[32] T.C. Pataky, One-dimensional statistical parametric mapping in Python, Comput. Methods Biomech. Biomed. Engin. 15 (2012) 295–301, https://doi.org/10.1080/10255842.2010.527837.
[33] T.C. Pataky, Generalized n-dimensional biomechanical field analysis using statistical parametric mapping, J. Biomech. 43 (2010) 1976–1982, https://doi.org/10.1016/j.jbiomech.2010.03.008.
[34] T. Sugiyama, J.S. Price, L.E. Lanyon, Functional adaptation to mechanical loading in both cortical and cancellous bone is controlled locally and is confined to the loaded bones, Bone 46 (2010) 314–321, https://doi.org/10.1016/j.bone.2009.08.054.
[35] A. Carriero, A.F. Pereira, A.J. Wilson, S. Castagno, B. Javaheri, A.A. Pitsillides, et al., Spatial relationship between bone formation and mechanical stimulus within cortical bone: combining 3D fluorochrome mapping and poroelastic finite element modelling, Bone Rep. 8 (2018) 72–80, https://doi.org/10.1016/j.bonr.2018.02.003.
[36] B. Javaheri, A. Carriero, M. Wood, R. De Souza, P.D. Lee, S. Shefelbine, et al., Transient peak-strain matching partially recovers the age-impaired mechanoadaptive cortical bone response, Sci. Rep. 8 (2018), https://doi.org/10.1038/s41598-018-25084-6.
[37] J.C. Fritton, E.R. Myers, T.M. Wright, M.C. van der Meulen, Bone mass is preserved and cancellous architecture altered due to cyclic loading of the Mouse tibia after orchidectomy, J. Bone Miner. Res. 23 (2008) 663–671, https://doi.org/10.1359/JBMR.080104.
[38] H. Yang, R.E. Embry, R.P. Main, Effects of loading duration and short rest insertion on cancellous and cortical bone adaptation in the mouse tibia, PLoS One 12 (2017) e0169519, , https://doi.org/10.1371/journal.pone.0169519.
[39] J. Xiong, M. Onal, R.L. Jilka, R.S. Weinstein, S.C. Manolagas, C.A. O'Brien, Matrix-embedded cells control osteoclast formation, Nat. Med. 17 (2011) 1235–1241, https://doi.org/10.1038/nm.2448.
[40] A.G. Robling, P.J. Niziolek, L.A. Baldridge, K.W. Condon, M.R. Allen, I. Alam, et al., Mechanical stimulation of bone in vivo reduces osteocyte expression of Sost/sclerostin, J. Biol. Chem. 283 (2008) 5866–5875, https://doi.org/10.1074/jbc.M705092200.
[41] S.D. Tan, T.J. de Vries, A.M. Kuijpers-Jagtman, C.M. Semeins, V. Everts, J. Klein-Nulend, Osteocytes subjected to fluid flow inhibit osteoclast formation and bone resorption, Bone 41 (2007) 745–751, https://doi.org/10.1016/j.bone.2007.07.019.
[42] J. Klein-Nulend, C.M. Semeins, N.E. Ajubi, P.J. Nijweide, E.H. Burger, Pulsating fluid flow increases nitric oxide (NO) synthesis by osteocytes but not periosteal fibroblasts - correlation with prostaglandin upregulation, Biochem. Biophys. Res. Commun. 217 (1995) 640–648, https://doi.org/10.1006/bbrc.1995.2822.
[43] B. Cheng, Y. Kato, S. Zhao, J. Luo, E. Sprague, L.F. Bonewald, et al., PGE2 is essential for gap junction-mediated intercellular communication between osteocyte-like MLO-Y4 cells in response to mechanical strain, Endocrinology 142 (8) (Aug 1 2001) 3464–3473, https://doi.org/10.1210/endo.142.8.8338.
[44] R.J. Van't Hof, S.H. Ralston, Cytokine-induced nitric oxide inhibits bone resorption by inducing apoptosis of osteoclast progenitors and suppressing osteoclast activity, J. Bone Miner. Res. 12 (1997) 1797–1804, https://doi.org/10.1359/jbmr.1997.12.11.1797.
[45] A.F. Pereira, B. Javaheri, A.A. Pitsillides, S.J. Shefelbine, Predicting cortical bone adaptation to axial loading in the mouse tibia, J. R. Soc. Interface 12 (2015) 20150590, , https://doi.org/10.1098/rsif.2015.0590.
[46] A. Carriero, L. Abela, A.A. Pitsillides, S.J. Shefelbine, Ex vivo determination of bone tissue strains for an in vivo mouse tibial loading model, J. Biomech. 47 (2014) 2490–2497, https://doi.org/10.1016/j.jbiomech.2014.03.035.